Simulation of the Dynamic Behavior of Deep Bed Filters

A simulation procedure for predicting the dynamic behavior of a deep bed filter over the entire practicable range of filter operation is developed. The method is based on synthesizing available quantitative results relating to filtration, and to porous media flows, within an overall framework which views the process to consist of two principal stages dominated by appropriate limiting deposition modes. Evaluation of the results through comparison with available data indicates, to the extent the nature of these types of data permits, that the method is surprisingly effective and even capable of predicting on satisfactorily quantitative basis some intricate details of observed filter behavior.

CHI TIEN
RAFFI M. TURIAN
and
HEMANT PENDSE

Department of Chemical Engineering and Materials Science
Syracuse University
Syracuse, New York 13210

SCOPE

This work is concerned with the development of a simulation procedure capable of predicting the dynamic behavior of a deep bed filter over the broadest practicable range of the pertinent variables involved, including, in particular, the value of the specific deposit. The method presented here was developed by assimilating available quantitative results relating to porous media flows, and to filtration, in the context of a conceptual framework which views the process, and its progressive evolution, to consist of two consecutive stages, each dominated by an appropriate limiting deposition mode. This picture of the process is supportable on the basis of observed filter behavior and does, moreover, provide the means for integrating results based on the two main collector types (the spherical and the constricted tube models) into the overall simulation scheme. The method we present incorporates the transformation, first suggested by Herzig et al. (1970), which reduces the governing conservation equations into a set of ordinary differential equations, thereby leading to considerable savings in computational effort.

CONCLUSIONS AND SIGNIFICANCE

Deep bed filtration is a subject which has, in recent years, developed a rich and varied literature. Despite the dramatic progress in our understanding which this has produced, a comprehensive method capable of predicting the dynamic behavior of a filter over its entire operational span has remained out of reach. No doubt the uncertainties surrounding some aspects of the nature of the deposition process, particularly the critical ones relating to the nature of the distribution of the deposited matter within the media and its evolution with progressive deposition, have stood as the main impediments obstructing progress towards such a general predictive scheme. In this work this problem is resolved by postulating an overall picture of the filtration process which views it to consist of two consecutive stages: a first stage dominated by deposition according to a smooth coating mode and assumed to endure until the specific deposit attains a prescribed transition value, followed by a second stage corresponding to transition to deposition by the constriction clogging mode. This picture of the process, though somewhat idealized, is in the main consistent with observed filter behavior. However, besides being conceptually consistent in this way, this overall deposition hypothesis provides a logical framework for incorporation into the simulation scheme of the two main collector types (the spherical and the constricted tube models) wherever each is appropriately applicable and thereby avails the method of the broad range of quantitative results developed relative to porous media flows and to filtration. An additionally significant feature of the present method is that the results in it have been cast in a form suitable for exploiting the enormous computational advantages resulting from the Herzig et al. (1970) transformation which reduces the governing conservation equations to a set of ordinary differential equations. The results of comparisons of predictions from the present scheme with available experimental filtrate quality and pressure drop history data suggest, to the extent that the nature of these types of filtration experiments permit, that the method is surprisingly effective. Indeed, the method is capable of predicting some rather intricate details of observed behavior and is suitable as a basis for filter design.

Deep bed filtration is an engineering operation in which the removal of suspended particulate and colloidal matter in a fluid stream is effected by passing the stream through porous media composed of granular substances. The main indicators of the dynamic behavior of the operation are the filtrate quality history and also the pressure drop history required to maintain a uniform throughput. The first defines the effectiveness and the capacity of the filter bed, and the second determines the length of the filter run.

The importance of an accurate simulation of the dynamics of deep bed filtration is evident, since it provides

Chi Tien is presently at the Department of Chemical Engineering, Texas Tech University, Lubbock, Texas 79409.

0001-1541-79-2396-0385-$01.25.

the basis for rational design and optimization. Ives (1960) proposed that filter performance can be described by using a macroscopic material balance equation together with an appropriate rate expression, and the pressure drop across the bed is then calculated using the Carman-Kozeny equation corrected for the clogging of bed due to deposition. Subsequent studies (Ives, 1963, 1969; Deb, 1969; Mohanka, 1969; Herzig et al., 1970; Wnek, Gidaspow, and Wasan, 1975) have been concerned with extensions, as well as refinements, of this approach and have included proposals for different forms of expressions for both filtrate rate and pressure drop. Among these works, that of Herzig et al. (1970) is particularly noteworthy for its inclusion of a procedure which results in a reduction of the pertinent equations (the macroscopic material balance and rate equations) to a set of two ordinary differential equations whose integration can be carried out without complicated algorithms. With the exception of the work by Wnek et al. (1975), however, the rate expressions used for filtration by all the studies cited above, as well as the pressure gradient expressions from which the overall pressure drop is calculated, contain adjustable model parameters or functional relationships which must be determined experimentally.

The work of Wnek et al. (1975) represents a departure from previous approaches inasmuch as it consists of an attempt to simulate filter performance on a predictive basis. In this work, the results of Yao et al. (1971) were used to calculate the rate of filtration, and, in addition, as part of the phenomenological description, a charge balance was made in order to account for the altered surface interaction resulting from the deposition of the colloidal matter. The effect of particle deposition was considered on the basis of the assumption that particle deposits form a relatively smooth coating around the filter grains. While this particular deposit morphology may be suitable for the filtration of fine colloidal suspensions, the assumption cannot be accepted generally as has been observed in the recent work of Pendse et al. (1977).

In contrast to the rational approach followed in the foregoing studies, an alternative method is the use of statistical models for the simulation of filter performance. Using data obtained from the filtration of ferric floc in a shallow filter bed, Hsiung (1967) and Hsiung and Cleasby (1968) developed a statistical filtration model and established extensive performance curves. Optimum design based on these results has been successful (Huang and Bauman, 1971; Conley and Hsiung, 1969), but the limitations of the approach derive from the need for the prior availability of the relevant experimental data and the associated difficulties.

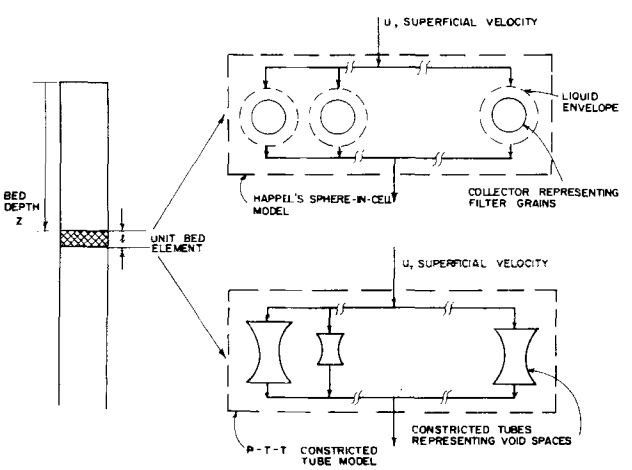

Fig. 1. Porous media representation.

In the present work, we develop a new method of simulation which differs from that of Wnek et al. in several important aspects. One principal distinction here consists of the use of a different method, based on a more recent theoretical calculation (Rajagopalan and Tien, 1976), for estimating the filter coefficient. Another distinction relates to the fact that by carrying out a more complete development of the effect of particle deposition on filter performance, we introduce the method of Herzig et al. (1970) in the simulation, instead of the more complicated Runge-Kuttta scheme used in their work. Most importantly, however, is the fact that the significance of the nature of the deposit morphology, and its possible evolution with progressive deposition, is recognized, and its effects are included in the present simulation method.

PHENOMENOLOGICAL DESCRIPTION OF DEEP BED FILTRATION

The basic equations describing the dynamic behavior of a deep bed filter are taken to be the following:

$$u\frac{\partial c}{\partial z}+\frac{\partial \sigma}{\partial \theta}=0 \tag{1}$$

$$\frac{\partial \sigma}{\partial \theta}=(u)\lambda c \tag{2}$$

$$\Delta p=p_{\text{out}}-p_{\text{in}}=\int_o^L\left(\frac{\partial p}{\partial z}\right)dz \tag{3}$$

$$\theta=t-\int_o^z\frac{\epsilon}{u}dz \tag{4}$$

$$\epsilon=f(\epsilon_o,\sigma) \tag{5}$$

$$c=c_o,\quad z=0 \tag{6}$$

$$c=c_i(z)\quad z>0,\quad \theta\leqq 0 \tag{7}$$

$$\sigma=\sigma_i(z)\quad z>0,\quad \theta\leqq 0 \tag{8}$$

Equation (1) is the macroscopic material balance for the suspended matter. Equation (2) can be considered as the definition of the filter coefficient, and the requirement that rate expressions reducible to, or consistent with, this form is implicitly assumed.

Filtration is an inherently transient process, since particle deposition almost inevitably must alter the structure of the filter medium. Therefore, consideration of the effects of particle deposition on filter performance constitutes a critical requirement in the study of deep bed filtration. In order to account for the changing media structure on both the rate of filtration and the flow within it, one takes

$$\lambda=\lambda_o F_1(\alpha,\sigma) \tag{9}$$

$$\frac{(\partial p/\partial z)}{(\partial p/\partial z)_o}=F_2(\beta,\sigma) \tag{10}$$

where α and β are parameter vectors characterizing the effects of particle deposits on the filter coefficient and on the pressure gradient, respectively.

In principle, the solution of Equation (1) to (3), subject to prescribed initial and boundary conditions [Equations (6) to (8)], provides a complete description of the dynamic behavior of the deep bed filter. However, in order to do so, it is first necessary to establish the relevant parameter values and the functional relationships contained in these equations [that is, λ_o, $f(\epsilon_o, \sigma)$ and

$F_1(\alpha, \sigma)$, and $F_2(\beta, \sigma)$]. The development of predictive methods for determining these quantities forms the core of the present work.

MODEL REPRESENTATION OF FILTER BED

To provide a physically realistic model as the basis for quantitive descriptions of the various processes of interest which occur in the porous medium, we use the concept of unit bed element (UBE) and of the unit collector proposed by Payatakes et al. (1973). Thus, the filter bed is postulated to consist of a number of unit bed elements, with a physical height of l, and connected in series. Each unit bed element in turn is assumed to consist of a number of particle collectors. The capacity of the bed to remove particulate matter can thus be described by the collection efficiency of the unit bed element η which is defined as the fraction of suspended particles entering the UBE removed. λ and η are related by the expression

$$\lambda = \left(\frac{1}{l}\right) \ln \frac{1}{1-\eta} \tag{11}$$

A schematic representation of the unit bed element is given in Figure 1.

Specification of the particular collector configurations in a unit bed element is admittedly somewhat arbitrary. In their earliest work, Payatakes et al. (1973) assumed these collectors to consist of constricted tubes of various size (unit cells). A number of other investigators however, (Yao et al., 1971; Spielman and FitzPatrick, 1973; Rajagopalan and Tien, 1976, 1977) have assumed them to be comprised of spheres of identical size.* The advantage of the collector model of Payatakes et al. resides in the fact that the constricted tube configuration embodies the convergent-divergent flow characteristics inherent to porous media flows. Furthermore, by taking the flow to be an internal one (in contrast to the external flow implicit in the spherical configuration), the effect of the neighboring grains upon each other can be accounted for, thus enabling, for example, consideration of the possibility that certain parts of the filter bed may become blocked. On the other hand, because use of the spherical collector leads to significant simplifications, it remains as an attractive alternative collector configuration, affording considerable computational convenience as well as leading to physically meaningful results when used in the appropriate context. Of particular significance to the present work, moreover, is the discovery in a recent study involving spherical collectors (Rajagopalan and Tien, 1976) that the theoretically calculated collection efficiency can be correlated, through a relatively simple relation, with the relevant dimensionless groups on which it depends. An additionally relevant finding in the Rajagopalan and Tien study is that the calculated collection efficiency values based on different collector configurations turn out to be comparable in magnitude.

As a consequence of the foregoing considerations, we propose to use a combination of the spherical and constricted tube configurations in this work. Briefly speaking, the spherical configuration will be used to estimate the rate of particle deposition, while the constricted tube configuration will be used to characterize the effect of particle deposition. Happel's porous media model, on which the work of Rajagopalan and Tien (1976) was based, contains two model parameters: a, the sphere diameter, and b, the dimension of the outer liquid shell. These are related to the media properties through the following equations:

$$a = d_g \tag{12}$$

$$b = \frac{a}{(1-\epsilon)^{1/3}} \tag{13}$$

The Payatakes-Tien-Turian model (1973a) assumes that for a unit bed element of unit cross-sectional area, there are N constricted tubes (or unit cells) of various sizes, with a distribution governed by certain determinable functions. In the present work, simplifications will be made by assuming that the unit cells are of the same size. For the present work, the important model variables are N, the constriction dimension of the unit cells d_c, and the physical length of the UBE, l. They are given by

$$N = \frac{6\epsilon^{1/3}(1-S_{wi})^{1/3}(1-\epsilon)^{2/3}}{\pi d_g^2} \tag{14}$$

$$d_c = 0.35\, d_g \tag{15}$$

$$l = \left[\frac{\pi}{6(1-\epsilon)} d_g^3\right]^{1/3} \tag{16}$$

Hypothesis of Deposition Process and Deposit Morphology

Consider an initially clean filter medium in which a fluid stream containing suspended particulate matter is passed. Initially, particle deposition takes the form of the adhesion of individual particles to the filter grains. As the operation is continued, deposition of particles on previously deposited ones, leading to formation of aggregates, becomes progressively more prevalent. The hydrodynamic drag force acting on these particle aggregates increases greatly as their size increases. Eventually, all or part of the aggregates may become reentrained and may even become redeposited within other parts of the bed. The redeposition of these, as aggregates of sufficiently large size, is mainly responsible for the blocking of pore constrictions. Eventually, the filter will either become completely clogged or reach a stage where the effect of reentrainment counterbalances that of deposition, and the bed becomes nonretentive.

In principle, a comprehensive filtration theory should provide a detailed quantitative description of every aspect of the deposition process, including the deposition rate, the deposit morphology, the reentrainment and redeposition effects, and so on. Such a theory is not yet available. In the present study, we develop a simulation of the dynamic behavior of deep bed filters by viewing the process to consist of the following two main stages, subject to the following assumptions:

1. In the two-stage deposition process considered here, the first stage is one in which deposition occurs primarily through the direct adhesion of individual particles to filter grains. The consequence of this mode of deposition is the formation of a relatively smooth layer of deposits outside filter grains. This first stage will continue until the local specific deposit σ reaches a transition value σ_{tran}.

2. The second stage of the deposition process is dominated by the formation of particle aggregates, the reentrainment of part of these aggregates, and their redeposition into constriction pores. Thus, the consequence of the processes prevailing in this second stage of deposition is the blocking of certain parts of the filter bed.

The second stage will continue until the reduced area available for flow leads to a sufficient increase of the interstitial velocity that the bed becomes nonretentive.

* The distinctions among them, however, usually involve the choice of the particular variant of the flow field around the spherical collector. The work of Rajagopalan and Tien (1976) uses a flow field similar to that of the Happel's model for porous media.

The termination of the second stage may or may not coincide with the complete clogging of the filter bed.

The necessity for using an assumed picture of the deposition process, as in the foregoing, arises because despite the fact that presently available information is adequate for a reasonable estimation of the rate of deposition on an overall basis, this information by itself is not sufficient to determine the effect of deposition on filter performance, as pointed out by Pendse et al. (1977). A complete description of the change of filter media structure requires information concerning both the extent of deposition as well as the nature of the deposit morphology. The deposition process portrayed above prescribes the dominant mode of deposit morphology for each of the two stages. The division of the filtration process into two distinct stages, and the more or less abrupt transition between deposition modes that it implies, may appear to be rather arbitrary. Nevertheless, there are some important justifications for it, and these will be brought up in later sections.

EFFECT OF DEPOSITION ON FILTER PERFORMANCE

The assumptions given above permit quantitative consideration of the effect of deposition as it changes with the extent of deposition expressed by σ. During the first stage, since deposition morphology is of the smooth coating mode, the net effect of deposition is to increase the effective grain size and to decrease the bed porosity. A clogged bed differs from that in the clean state by the increased value of d_g and the decreased value of ϵ. The changes in these are expressed by

$$\epsilon = \epsilon_o - \frac{\sigma}{1-\epsilon_d} \tag{17}$$

$$\frac{d_g}{d_{go}} = \left(\frac{1-\epsilon}{1-\epsilon_o}\right)^{1/3} \tag{18}$$

$$\frac{V}{V_o} = \frac{\epsilon_o}{\epsilon} \tag{19}$$

Equation (17) expresses the change of local porosity in terms of the local specific deposit. Note that in the macroscopic conservation equation [Equation (1)], σ refers to the actual volume of the deposited particles. The deposited layer of particles will, in general, possess its own characteristic porosity, and this is designated by ϵ_d here. The specification of this value will be discussed later. Equations (17) to (19) apply until σ reaches its transition value σ_{tran}.

During the second stage, the deposition is assumed to be of the blocking mode; that is, the lodging of particle aggregates in pore constrictions due to reentrainment and redeposition. Accordingly, the effect of deposition can most conveniently be viewed if the filter media is assumed to be described by the Payatakes-Tien-Turian model. The extent of deposition is related to the change in the value of N, which can be expressed as a function of σ through the equation

$$N = N_o - \frac{l(\sigma - \sigma_{\text{tran}})}{(\beta)\frac{\pi}{6}d_c^3(1-\epsilon_d)} \tag{20}$$

Equation (20) is based upon the following reasoning. The quantity $(\beta)(\pi/6)d_c^3(1-\epsilon_d)$ represents the average amount of particle aggregates required to block off a unit cell. In this, $(\pi/6)d_c^3(1-\epsilon_d)$ is the minimum size of a particle aggregate which can be lodged in the pore constriction of size d_c to effect complete clogging, if the aggregate can be approximated as a spherical body. β is a parameter to account for the possibility that the actual deposit causing the blockage is in excess of the minimum required amount. The assignment of a numerical value to β will be discussed later. However, N_o should be evaluated at conditions corresponding to those existing at the end of the first stage; that is

$$N_o = \frac{6\epsilon_{\text{tran}}^{1/3}(1-s_{wi})(1-\epsilon_{\text{tran}})^{2/3}}{\pi(d_g)^2_{\text{tran}}} = 6\frac{\epsilon_{\text{tran}}^{1/3}(1-s_{wi})(1-\epsilon_o)^{2/3}}{\pi d_{go}^2} \tag{21}$$

Equation (20) can be rewritten as

$$\frac{N}{N_o} = 1 - \frac{(\sigma-\sigma_{\text{tran}})l}{N_o\beta\left(\frac{\pi}{6}\right)d_c^3(1-\epsilon_d)} \tag{22}$$

It must be noted that during the second stage, the dimension of the functioning collectors within the unit bed element will remain unchanged from the value attained at the end of the first stage; that is

$$d_g = (d_{go})\left(\frac{1-\epsilon_{\text{tran}}}{1-\epsilon_o}\right)^{1/3} \tag{23}$$

The termination of the second stage comes when the interstitial velocity V reaches or exceeds the critical value V_{cr}. The corresponding value of σ at that point, designated by σ_{ult}, can be found from the fact that V is inversely proportional to N, or

$$\frac{1}{\left[1-\frac{\sigma_{\text{tran}}}{(1-\epsilon_d)\epsilon_o}\right]}\left(\frac{V_o}{V_{cr}}\right) = \frac{N_{\text{ult}}}{N_o} = 1 - \frac{(\sigma_{\text{ult}}-\sigma_{\text{tran}})l}{N_o\beta\left(\frac{\pi}{6}\right)d_c^3(1-\epsilon_d)} \tag{24}$$

ESTIMATION OF MODEL PARAMETER AND FUNCTIONAL RELATIONSHIPS

Pressure Gradient Expression $F_2(\beta,\sigma)$

To obtain the overall pressure drop across a filter bed for a given flow rate, Equations (3) and (10) can be used to give

$$\Delta p = \left(\frac{\partial p}{\partial z}\right)_o \int_o^L F_2(\beta,\sigma)\,dz \tag{25}$$

The pressure gradient of clean filter beds can be estimated from the classical Carman-Kozeny equation:

$$-\left(\frac{\partial p}{\partial z}\right)_o = \frac{150\mu}{d_{go}^2}(V_o)\frac{(1-\epsilon_o)^2}{\epsilon_o^2} \tag{26}$$

During the first stage, when the deposit morphology obeys the smooth coating mode, deposition merely changes the effective grain size, the porosity, and indirectly the interstitial velocity. Thus, one has

$$F_2(\beta,\sigma) = F_{2,s}(\beta,\sigma) = \frac{(\partial p/\partial z)}{(\partial p/\partial z)_o} = \left(\frac{d_{go}}{d_g}\right)^2\frac{\epsilon_o^3(1-\epsilon)^2}{\epsilon^3(1-\epsilon_o)^2} \tag{27}$$

Combining Equations (27) together with (17), (18),

and (19), we get

$$F_2(\beta,\sigma) = F_{2,s}(\beta,\sigma) = \left[1 - \frac{\sigma}{\epsilon_o(1-\epsilon_d)}\right]^{-3} \left[1 + \frac{\sigma}{(1-\epsilon_o)(1-\epsilon_d)}\right]^{4/3} \quad \text{for} \quad \sigma \leq \sigma_{\text{tran}} \tag{28}$$

During the second stage, the result of deposition is to reduce the number of unit cells available for flow. The interstitial velocity V for the unit cells which remain open becomes

$$\frac{V}{V_{\text{tran}}} = \frac{N_o}{N} = \left[1 - \frac{6(\sigma - \sigma_{\text{tran}})l}{N_o \pi d_c^3 \beta(1-\epsilon_d)}\right]^{-1} \tag{29}$$

As far as the pressure gradient expression is concerned, it is important to realize that for those parts of the bed which remain open, the media structure is the same as that at the end of the first stage. Therefore, the only relevant variable which undergoes a change resulting from the increasing deposition is the interstitial velocity. Accordingly

$$\frac{(\partial p/\partial z)}{(\partial p/\partial z)_{\sigma_{\text{tran}}}} = \left[1 - \frac{6(\sigma - \sigma_{\text{tran}})l}{N_o \pi d_c^3 \beta(1-\epsilon_d)}\right]^{-1} \tag{30}$$*

or

$$F_2(\beta,\sigma) = F_{2,b}(\beta,\sigma) = \frac{(\partial p/\partial z)}{(\partial p/\partial z)_o} = F_{2,s}(\beta,\sigma_{\text{tran}}) \times \frac{(\partial p/\partial z)}{(\partial p/\partial z)_{\sigma_{\text{tran}}}} = \left[1 - \frac{\sigma_{\text{tran}}}{\epsilon_o(1-\epsilon_d)}\right]^{-3} \left[1 + \frac{\sigma_{\text{tran}}}{(1-\epsilon_o)(1-\epsilon_d)}\right]^{4/3} \left[1 - \frac{6(\sigma - \sigma_{\text{tran}})l}{N_o \pi d_c^3 \beta(1-\epsilon_d)}\right]^{-1} \quad \sigma > \sigma_{\text{tran}} \tag{31}$$

Initial Filter Coefficient λ_0 and the Filter Coefficient Expression $F_1(\alpha,\sigma)$

The filter coefficient λ and the collection efficiency of the unit bed element η are related through Equation (11):

$$\lambda = \frac{1}{l} \ln \frac{1}{1-\eta} \tag{11}$$

For the proposed method, the individual collectors are assumed to be identical and spherical. The collection efficiency of the unit bed element then becomes the same as individual collector, and Equation (11) can be rewritten to yield

$$\lambda = \frac{3(1-\epsilon)}{2d_g} \ln \frac{1}{1-\eta} \simeq \frac{3(1-\epsilon)}{2d_g} \cdot \eta \quad \text{(for small } \eta\text{)} \tag{32}$$

The expression obtained by Rajagopalan and Tien (1976) correlating collection efficiencies, obtained from trajectory calculations for a porous medium described by Happel's model with the relevant dimensionless groups representing the various deposition mechanisms, will be used to calculate the filter coefficient. This expression is given by

$$\eta = (1-\epsilon)^{2/3} A_s N_{Lo}^{1/8} N_R^{15/8} + 3.375 \times 10^{-3}(1-\epsilon)^{2/3} A_s N_G^{1.2} N_R^{-0.4} + 4A_s^{1/3} N_{Pe}^{-2/3} \tag{33}$$

with

$$N_{Lo} = \frac{4H}{9\pi\mu d_p^2 U} \tag{34}$$

$$N_R = \frac{d_p}{d_g} \tag{35}$$

$$N_G = \frac{(\rho_p - \rho) d_p^2 g}{18\pi\mu U} \tag{36}$$

$$N_{Pe} = \frac{3\pi\mu d_p d_g U}{kT} \tag{37}$$

$$A_s = \frac{2(1-p^5)}{w} \tag{38}$$

$$p = (1-\epsilon)^{1/3} \tag{39}$$

$$w = 2 - 3p + 3p^5 - 2p^6 \tag{40}$$

Equation (33) is valid for $N_R < 0.18$ and for the case wnen the surface interaction is favorable. It is applicable to both clean and clogged filter beds, provided proper values of relevant quantities are used to account for the effect of deposition.

During the first stage, since the effect of deposition is to change the size of the grain and to alter the porosity of the bed,* both N_G and N_{Lo} remain unchanged. Accordingly, one has

$$\frac{\eta}{\eta_o} = B_1 \left(\frac{1-\epsilon}{1-\epsilon_o}\right)^{2/3} \frac{A_s}{A_{so}} \left(\frac{d_{go}}{d_g}\right)^{15/8} + B_2 \left(\frac{1-\epsilon}{1-\epsilon_o}\right)^{2/3} \left(\frac{A_s}{A_{so}}\right) \left(\frac{d_g}{d_{go}}\right)^{0.4} + B_3 \left(\frac{A_s}{A_{so}}\right)^{1/3} \left(\frac{dg}{d_{go}}\right)^{-2/3} \tag{41}$$

where

$$B_1 = \frac{(1-\epsilon_o)^{2/3}}{\eta_o} A_{so} \cdot N_{Lo}^{1/8} \cdot N_{R_o}^{15/8} \tag{42}$$

$$B_2 = \frac{3.375 \times 10^{-3}}{\eta_o} (1-\epsilon_o)^{2/3} A_{so} \cdot N_G^{1.2} \cdot N_{R_o}^{-0.4} \tag{43}$$

$$B_3 = \frac{4 A_{so}^{1/3} N_{Pe_o}^{-2/3}}{\eta_o} \tag{44}$$

Moreover, based on Equation (32), we have (for $\eta \ll 1$)

$$\frac{\lambda}{\lambda_o} = \left(\frac{d_{go}}{d_g}\right)\left(\frac{1-\epsilon}{1-\epsilon_o}\right)\frac{\eta}{\eta_o} \tag{45}$$

The filter coefficient expression $F_1(\alpha, \sigma)$ is, therefore, given by

$$F_1(\alpha,\sigma) = F_{1,s}(\alpha,\sigma) = B_1 \frac{A_s}{A_{so}} \left(\frac{1-\epsilon}{1-\epsilon_o}\right)^{17/24} + B_2 \left(\frac{A_s}{A_{so}}\right)\left(\frac{1-\epsilon}{1-\epsilon_o}\right)^{\frac{4.4}{3}} + B_3 \left(\frac{A_s}{A_{so}}\right)^{1/3} \left(\frac{1-\epsilon}{1-\epsilon_o}\right)^{4/9}$$

$$= B_1 \frac{A_s}{A_{so}} \left[1 + \frac{\sigma}{(1-\epsilon_o)(1-\epsilon_d)}\right]^{17/24} + B_2 \left(\frac{A_s}{A_{so}}\right) \left[1 + \frac{\sigma}{(1-\epsilon_o)(1-\epsilon_d)}\right]^{\frac{4.4}{3}} + B_3 \left(\frac{A_s}{A_{so}}\right)^{1/3}$$

* These results can be seen more directly from the work of Payatakes et al. (1973*b*). The pressure gradient is proportional to the pressure drop across a unit cell. For creeping flow, the pressure drop across a unit cell is proportional to the interstitial velocity.

* The approach velocity U, however, remains the same and is equal to u. The flow field, however, is changed, since the ratio of a/b, where b is the diameter of liquid envelope, is increased.

$$\left[1+\frac{\sigma}{(1-\epsilon_o)(1-\epsilon_d)}\right]^{4/9} \quad \text{for} \quad \sigma<\sigma_{\text{tran}} \tag{46}$$

During the second stage, for those parts of the bed remaining open, the dimension of the equivalent collector and the porosity do not change. The approach velocity will increase as the extent of clogging increases. Since the approach velocity during the first stage is the same as the superficial velocity (volumetric rate divided by the cross-section area of bed), the ratio U/U_o is given as

$$\frac{U}{U_o}=\frac{N_o}{N}=\left[1-\frac{(\sigma-\sigma_{\text{tran}})l}{N_o\beta\left(\frac{\pi}{6}\right)d_c^3(1-\epsilon_d)}\right]^{-1} \tag{47}$$

Accordingly, the ratio of λ to $\lambda_{\sigma_{\text{tran}}}$ becomes

$$\begin{aligned}\frac{\lambda}{\lambda_{\sigma_{\text{tran}}}}=\frac{\eta}{\eta_{\sigma_{\text{tran}}}}&=\frac{(1-\epsilon)^{2/3}A_sN_{Lo}{}^{1/8}N_R{}^{15/8}|}{\eta_{\sigma_{\text{tran}}}}\sigma_{\text{tran}}\left(\frac{U}{U_o}\right)^{-1/8}\\&+\frac{3.375\times10^{-3}(1-\epsilon)^{2/3}A_sN_G{}^{1/2}N_R{}^{-0.4}|}{\eta_{\sigma_{\text{tran}}}}\sigma_{\text{tran}}\left(\frac{U}{U_o}\right)^{-1/2}\\&+\frac{4A_s{}^{1/3}N_{Re}{}^{-2/3}|}{\eta_{\sigma_{\text{tran}}}}\sigma_{\text{tran}}\left(\frac{U}{U_o}\right)^{-2/3}\\&=c_1\left[1-\frac{(\sigma-\sigma_{\text{tran}})l}{N_o\beta\left(\frac{\pi}{6}\right)d_c^3(1-\epsilon_d)}\right]^{1/8}\\&=c_2\left[1-\frac{(\sigma-\sigma_{\text{tran}})l}{N_o\beta\left(\frac{\pi}{6}\right)d_c^3(1-\epsilon_d)}\right]^{1/2}\\&=c_3\left[1-\frac{(\sigma-\sigma_{\text{tran}})l}{N_o\beta\left(\frac{\pi}{6}\right)d_c^3(1-\epsilon_d)}\right]^{2/3}\end{aligned} \tag{48}$$

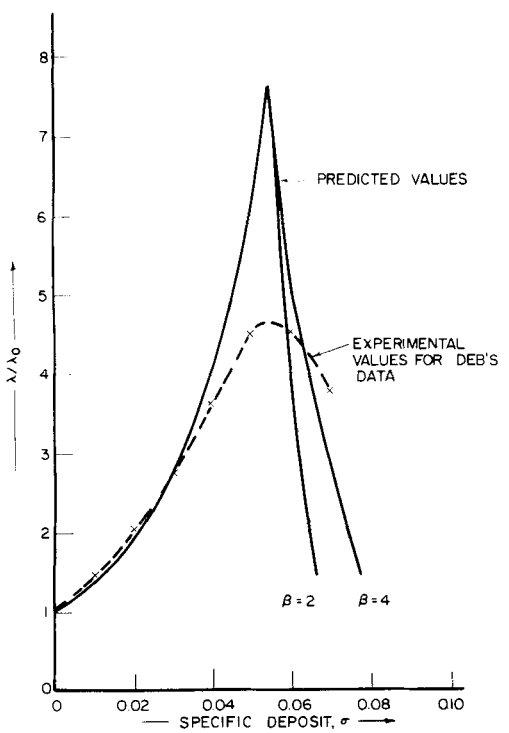

Fig. 2. Variation of filter coefficient with specific deposit.

$$c_1=\frac{B_1\left(\frac{A_{s,\text{tran}}}{A_{so}}\right)\left[1+\frac{\sigma_{\text{tran}}}{(1-\epsilon_o)(1-\epsilon_d)}\right]^{1/24}+B_2\left(\frac{A_{s,\text{tran}}}{A_{so}}\right)\left[1+\frac{\sigma_{\text{tran}}}{(1-\epsilon_o)(1-\epsilon_d)}\right]^{2.4/3}+B_3\left(\frac{A_{s,\text{tran}}}{A_{so}}\right)^{1/3}\left[1+\frac{\sigma_{\text{tran}}}{(1-\epsilon_o)(1-\epsilon_d)}\right]^{-2/9}}{B_1\left(\frac{A_{s,\text{tran}}}{A_{so}}\right)\left[1+\frac{\sigma_{\text{tran}}}{(1-\epsilon_o)(1-\epsilon_d)}\right]^{1/24}+B_2\left(\frac{A_{s,\text{tran}}}{A_{so}}\right)\left[1+\frac{\sigma_{\text{tran}}}{(1-\epsilon_o)(1-\epsilon_d)}\right]^{2.4/3}+B_3\left(\frac{A_{s,\text{tran}}}{A_{so}}\right)^{1/3}\left[1+\frac{\sigma_{\text{tran}}}{(1-\epsilon_o)(1-\epsilon_d)}\right]^{-2/9}} \tag{49}$$

$$c_2=\frac{B_2\left(\frac{A_{s,\text{tran}}}{A_{so}}\right)\left[1+\frac{\sigma_{\text{tran}}}{(1-\epsilon_o)(1-\epsilon_d)}\right]^{2.4/3}+B_3\left(\frac{A_{s,\text{tran}}}{A_{so}}\right)^{1/3}\left[1+\frac{\sigma_{\text{tran}}}{(1-\epsilon_o)(1-\epsilon_d)}\right]^{-2/9}}{B_1\left(\frac{A_{s,\text{tran}}}{A_{so}}\right)\left[1+\frac{\sigma_{\text{tran}}}{(1-\epsilon_o)(1-\epsilon_d)}\right]^{1/24}+B_2\left(\frac{A_{s,\text{tran}}}{A_{so}}\right)\left[1+\frac{\sigma_{\text{tran}}}{(1-\epsilon_o)(1-\epsilon_d)}\right]^{2.4/3}+B_3\left(\frac{A_{s,\text{tran}}}{A_{so}}\right)^{1/3}\left[1+\frac{\sigma_{\text{tran}}}{(1-\epsilon_o)(1-\epsilon_d)}\right]^{-2/9}} \tag{50}$$

$$c_3=\frac{B_3\left(\frac{A_{s,\text{tran}}}{A_{so}}\right)^{1/3}\left[1+\frac{\sigma_{\text{tran}}}{(1-\epsilon_o)(1-\epsilon_d)}\right]^{-2/9}}{B_1\left(\frac{A_{s,\text{tran}}}{A_{so}}\right)\left[1+\frac{\sigma_{\text{tran}}}{(1-\epsilon_o)(1-\epsilon_d)}\right]^{1/24}+B_2\left(\frac{A_{s,\text{tran}}}{A_{so}}\right)\left[1+\frac{\sigma_{\text{tran}}}{(1-\epsilon_o)(1-\epsilon_d)}\right]^{2.4/3}+B_3\left(\frac{A_{s,\text{tran}}}{A_{so}}\right)^{1/3}\left[1+\frac{\sigma_{\text{tran}}}{(1-\epsilon_o)(1-\epsilon_d)}\right]^{-2/9}} \tag{51}$$

$$F_1(\alpha, \sigma) = F_{1,b}(\alpha, \sigma) = F_{1,s}(\alpha, + \sigma_{tran}) \times \left[c_1 \left\{ 1 - \frac{6(\sigma - \sigma_{tran})l}{N_o \pi d_c^3 \beta (1 - \epsilon_d)} \right\}^{1/8} + c_2 \left\{ 1 - \frac{6(\sigma - \sigma_{tran})l}{N_o \pi d_c^3 \beta (1 - \epsilon_d)} \right\}^{1.2} + c_3 \left\{ 1 - \frac{6(\sigma - \sigma_{tran})l}{N_o \pi d_c^3 \beta (1 - \epsilon_d)} \right\}^{2/3} \right]$$

$$\text{for} \quad \sigma_{tran} < \sigma < \sigma_{ult} \tag{52}$$

and in addition

$$F_1(\alpha, \sigma_{ult}) = 0 \tag{53}$$

specifies that the function $F_1(\alpha, \sigma)$ is discontinuous at $\sigma = \sigma_{ult}$.

METHOD OF SIMULATION

The results of the work described above can be briefly summarized as follows:

$$u \frac{\partial c}{\partial z} = - \frac{\partial \sigma}{\partial \theta} = - (u \cdot \lambda_o) F_1(\alpha, \sigma) c \tag{54}$$

$$\Delta p = \left(\frac{\partial p}{\partial z} \right)_o \int_o^L F_2(\beta, \sigma) dz \tag{25}$$

$$F_1(\alpha, \sigma) = \begin{cases} F_{1,s}(\alpha, \sigma) & \text{for} \quad 0 < \sigma \leq \sigma_{tran} \\ F_{1,b}(\alpha, \sigma) & \text{for} \quad \sigma_{tran} < \sigma < \sigma_{ult} \\ 0 \quad \text{for} \quad \sigma = \sigma_{ult} \end{cases} \tag{55}$$

$$F_2(\beta, \sigma) = \begin{cases} F_{2,s}(\beta, \sigma) & \text{for} \quad 0 < \sigma \leq \sigma_{tran} \\ F_{2,b}(\beta, \sigma) & \text{for} \quad \sigma_{tran} < \sigma \leq \sigma_{ult} \end{cases} \tag{56}$$

$$c = c_o \quad \text{at} \quad z = 0, \quad \theta > 0 \tag{57}$$

$$c = 0, \quad \sigma = 0, \quad z > 0, \quad \theta < 0 \tag{58}$$

where $F_{1,s}$, $F_{1,b}$, $F_{2,s}$, and $F_{2,b}$ are given by Equations (46), (52), (28), and (31), respectively. The initial conditions are those of a clean filter (that is, free of any particulate matter).

Equations (54), (25), and (55) to (58) are the relevant equations and form the basis for the simulation of the dynamic behavior of deep bed filters. In the formulation of the problem, a number of quantities have been introduced, and these include ϵ_d, the deposit porosity (appearing in $F_{1,s}$, $F_{1,b}$, $F_{2,s}$ and $F_{2,b}$), β, the correction factor for the deposit required to block a pore constriction (appearing in $F_{1,b}$), σ_{tran}, which signifies the transition from the first stage to the second stage and σ_{ult} the ultimate specific deposit achieved. Definite values must be assigned to these quantities before these equations can be used to carry out filter performance calculations.

The value of ϵ_d is taken as 0.7. This particular choice is motivated by consideration of the results of a number of previous studies. Deb (1969) determined experimentally that the porosity of flocs formed from particulate matter commonly found in influent streams of deep bed filters under sedimentation has the value 0.75. A theoretical study by Hutchinson and Sutherland (1965) concerning the formation of floc from coagulation indicates that the flocs have a porosity of about 0.8. However, the porosity of a granular bed at the incipience of fluidization falls in the range between 0.45 and 0.6, depending upon the sphericity of the particles. The choice of 0.7, therefore, represents a reasonable compromise. The meaning of σ_{ult} suggests that when σ reaches this value, a dynamic equilibrium is established between deposition and reentrainment. Maroudas (1961) and Maroudas and Eisenclam (1965), based on studies with model and experimental filters, have shown that the nonretentive stage can be characterized by a critical interstitial velocity. Their results extrapolated to a granular bed of average grain size 500 μm, an initial porosity of 0.4, and average particle size 6 μm with linear flow rate ranging from 0.12 to 0.14 cm/s give to the ratio of the critical to initial interstitial velocity a value of approximately 40, or

$$\frac{V_{cr}}{V_o} = 40 \tag{59}$$

Thus, it is more convenient to determine the nonretentivity of a filter bed by the value of the interstitial velocity rather than the specific deposit. Since nonretentivity in all likelihood occurs in the second stage, the corresponding value of N_{ult} is, therefore

$$\frac{N_{ult}}{N_o} = \frac{V_{\sigma_{tran}}}{V_{cr}} \simeq \frac{1}{20} \tag{60}$$

on the basis that the value of $V_{\sigma_{tran}}$ is approximately two times the value of V_o for the bed in its clean state.

It is more difficult to estimate values for β and σ_{tran}, since there is little direct experimental evidence relating to them. Our use of the two-stage hypothesis was motivated by the fact that it is consistent with and does provide a correct prediction of observed λ vs. σ behavior (that is, λ first increases with σ then decreases, see Figure 2). A suitable choice for σ_{tran}, therefore, should correspond to the values of σ at which λ attains a maximum. Experimental values obtained by several investigators (Camp, 1964; Deb, 1969; Ives, 1961) indicate this maximum is reached at values of σ ranging from 0.04 to 0.06. Therefore, insofar as the available evidence justifies, a reasonable tentative value is given by

$$\sigma_{tran} = 0.05 \tag{61}$$

Only a rather coarse estimate for the value of β is possible presently. The maximum limit of σ can be calculated from Equation (17) by letting $\epsilon = 0$. This corresponds to the case when the entire pore space is filled with deposit, and thus

$$\sigma_{max} = (1 - \epsilon_d) \epsilon_o \tag{62}$$

A corresponding value of β can be found from Equation (22) by letting $N = 0$ and $\sigma = (\sigma)_{max}$. This limiting value of β is given by

$$(\beta)_{max} = \frac{[\sigma_{max} - \sigma_{tran}]l}{N_o \left(\frac{\pi}{6} \right) d_c^3 (1 - \epsilon_d)} \tag{63}$$

If one assumes that the clean bed porosity is about 0.4, and using the relevant expressions for the other quantities in Equation (63), $(\beta)_{max}$ is found to have a value on the order of 10. However, if we use the constricted tube configuration to represent the collectors, and appeal to the basic assumption that the blocking mode is effected through reentrainment and redeposition, it is unlikely that the lower half would become filled with deposits. Thus, the maximum value of $(\beta)_{max}$ is probably half that given by Equation (63), or about 5. The minimum value of β is one. Accordingly, as a rough approximation, it is tentatively taken to be 2.

The procedure developed by Herzig, Leclerc, and LeGoff (1970) can be applied to the solution of Equations (54), (55), (57), and (58). In essence, these

authors have shown that the partial differential equation system [Equations (1) and (2)] is equivalent to two ordinary differential equations given as

$$\frac{d\sigma_o}{d\theta} = (u\cdot\lambda_o\cdot c_o)F_1(\alpha, \sigma_o), \quad \theta > 0 \tag{64}$$

$$\sigma_o = 0, \quad \theta \leq 0 \tag{65}$$

$$\frac{d\sigma}{dz} = -\lambda_o F_1(\alpha,\sigma)\sigma \quad z > 0 \tag{66}$$

$$\sigma = \sigma_o \quad z = 0 \tag{67}$$

$$\frac{c}{c_o} = \frac{\sigma}{\sigma_o} \quad \theta > 0 \tag{68}$$

Accordingly, the history of the specific deposit at the inlet is solved first [Equations (64) and (65)], and these results can be used as initial conditions to obtain the specific deposit profile at different values of θ [Equation (66) and (67)]. The result is found to be

$$\int_o^{\sigma_o} \frac{dy}{F_1(\alpha,y)} = (u\cdot\lambda_o\cdot c_o)\theta \tag{69}$$

$$\int_{\sigma_o}^{\sigma} \frac{-dy}{yF_1(\alpha,y)} = (\lambda_o)(z) \tag{70}$$

Equations (69) and (70) give specific profiles at various times. These results can be used in conjunction with Equation (68) to calculate the effluent (or filtrate) quality. The integrals [Equations (69) and (70)] can be evaluated using a number of algorithms (trapezoidal rule, for example). The specific deposit is a monotonically increasing function of θ up to the point when it reaches its ultimate value, which can be calculated from the criteria given by Equation (60). Once this value is reached at the inlet, the specific deposit profile now is given as

For $\theta > \theta_{\text{onset}}$

$$\sigma = \sigma_{\text{ult}} \quad 0 < z < z_{\text{sat}} \tag{71}$$

and

$$\frac{d\sigma}{dz} = -\lambda_o F_1(\alpha,\sigma)\sigma \quad z > z_{\text{sat}} \tag{72}$$

$$\sigma = \sigma_{\text{ult}} \quad \text{at} \quad z = z_{\text{sat}} \tag{73}$$

The value of θ_{onset} is obtained from Equation (64), or

$$\theta_{\text{onset}} = \frac{\int_o^{\sigma_{\text{ult}}} \frac{dy}{F_1(\alpha,y)}}{u\lambda_o c_o} \tag{74}$$

The value of z_{sat} is clearly a function of θ. The relationship between z_{sat} and θ can be found from overall material balance, or

$$u(\theta - \theta_{\text{onset}})c_o = (z_{\text{sat}})\sigma_{\text{ult}}$$

or

$$z_{\text{sat}} = \frac{u(\theta - \theta_{\text{onset}})c_o}{\sigma_{\text{ult}}} \tag{75}$$

COMPARISON WITH EXPERIMENTAL DATA

A number of investigators have reported data on filter performance. They are used as a basis of comparison with the proposed simulation method. These data include those of Ives (1961), Camp (1964), Rimer (1968), and Deb (1969) obtained from experimental filters of various kinds. The particulates filtered ranged from algae and ferric floc to clays a few microns in size. Other experimental conditions are listed in Table 1.

The predictions of concentration profiles (that is, c vs. z and σ vs z at various times) were made from the integration of Equations (69) and (70) and the relationship of (68). The overall pressure drop Δp was obtained from Equation (25) with the knowledge of the specific deposit profile and the initial value of Δp from the Carman-Kozeny equation [that is, Equations (26)]. The integration was made using the trapezoidal rule. The increments used for integration were 0.305 cm and 360 s.

To make the prediction, the initial value of Δp calculated from Equation (26) was found invariably different from the experimental value. However, the difference is always rather slight (approximately 20%). The initial filter coefficient was calculated from Equations (32) and (33) with the exception of Deb's case. In this case, the calculated λ was found to be significantly different from the experimental value (by a factor of more than 2), and the experimental value was used instead. The value of σ_{tran} was taken to be the value of σ which corresponded to the maximum value in the λ vs. σ curve. However, this information was not provided in one of the four cases (that is, Rimer's), and σ_{tran} was set to be 0.05 as stated earlier. Two values of β(2 and 4) were used to give a range of predictions. Other model parameters (N_o, l, and d_c) and other experimental conditions necessary to the prediction are shown in Table 1 as stated earlier.

The comparison of concentration profiles was made against the data of Deb (1968), Ives (1961), and Camp (1964) and are shown in Figures 3, 4, and 5. The comparison with Ive's data is given in Figure 4 in which the values of σ vs. θ at various bed height are presented. The

TABLE 1. EXPERIMENTAL CONDITIONS AND MODEL PARAMETERS

Quantity	Deb (1969)	Ives (1961)	Camp (1964)	Rimer (1968)
Filter medium	Sand	Sand	Sand	Sand
Particles in suspension	Fuller's earth	Algae	Hydrous ferric oxide floc	Fe Cl_3 floc
Bed porosity, ϵ_o	0.43*	0.39*	0.41*	0.41*
Superficial velocity, u(cm/s)	0.13*	0.136*	0.136*	0.204*
Grain diameter, d_{g_o}(cm)	0.0493*	0.0511*	0.0514*	0.0460*
Particle diameter, d_p (cm)	0.0006*	0.00065†	0.00062*	0.0006††
Particle density, ρ_p(g/cm^3)	2.22*	2.0†	3.6†	3.6††
Feed concentration, $c(v/v)$	45×10^{-6}*	135×10^{-6}*	150×10^{-6}*	2.65×10^{-6}*
Transition sp. deposit, σ_{tran}	0.055**	0.04**	0.04**	0.05†
Number of constrictions, N_o (cm^{-2})	310††	311††	352††	435††
Length of UBE, l(cm)	0.0479††	0.0486††	0.0494††	0.0442††
Constriction diameter, d_c, (cm)	0.0192††	0.0193††	0.0184††	0.165††

* Reported values.
† Assumed values.
** These σ_{tran} values are based on empirical data on filter coefficient vs. sp. deposit.
†† Calculated values.

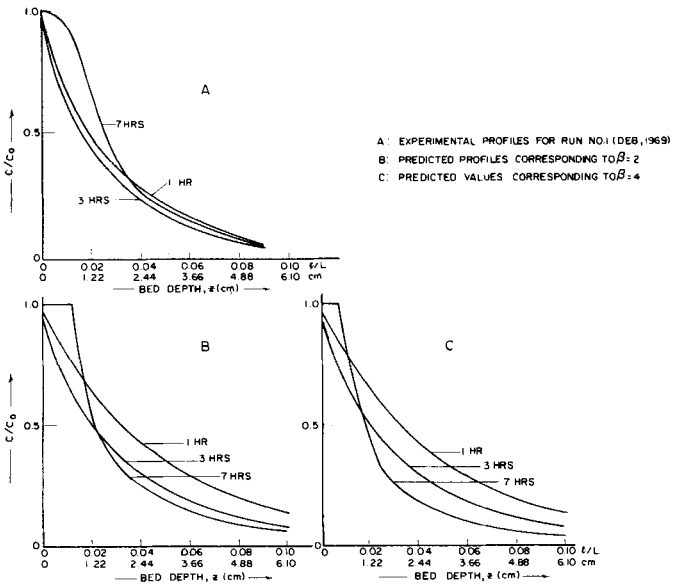

Fig. 3. Comparison of experimental and predicted concentration profiles. (Deb, 1969)

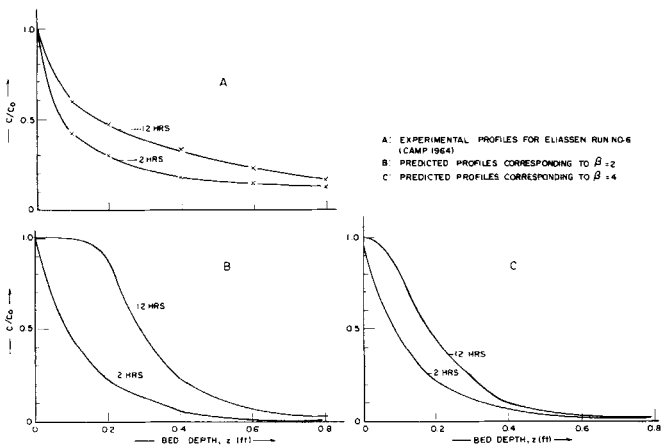

Fig. 5. Comparison of experimental and predicted concentration profiles. (Camp, 1964)

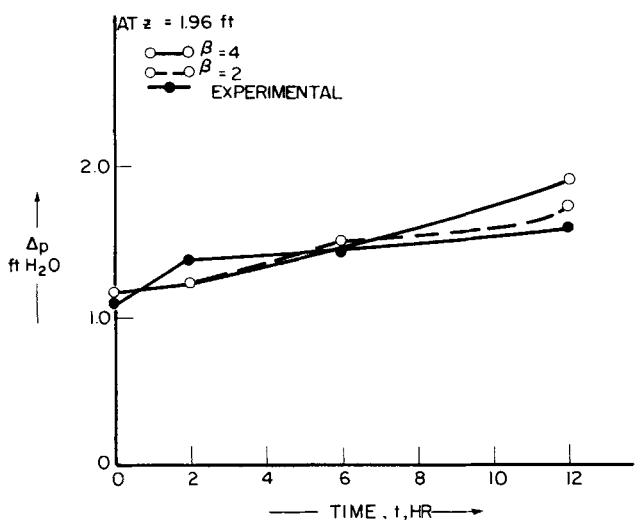

Fig. 7. Comparison of experimental and predicted values for pressure drop data (Camp, 1964).

predictions show that σ reached its ultimate value σ_{ult} as assumed in the simulation method. The value of σ_{ult} was found to be 0.062 for $\beta = 4$ and 0.053 for $\beta = 2$. The experimental data did not clearly show the achievement of this ultimate value, but if they had, the value would seemed to have to be substantially higher (above 0.07). In general, the agreement is only fair. However, this must be viewed in light of the fact that uncertainty associated with the experimental determination of the specific deposit in a filtration experiment is inherently large.

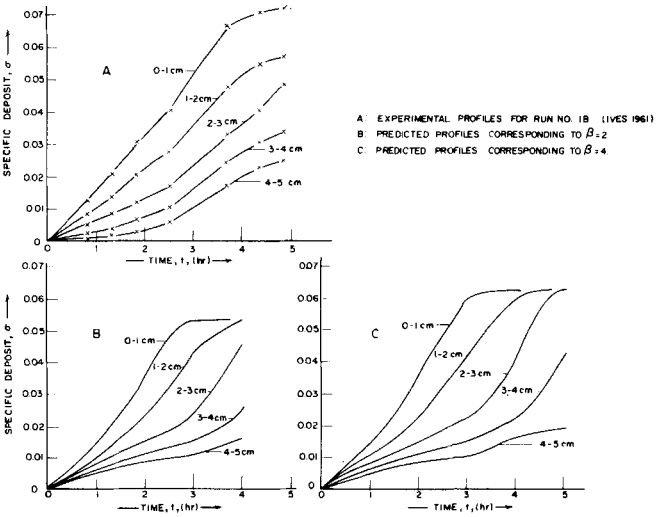

Fig. 4. Comparison of experimental and predicted specific deposit profiles. (Ives, 1961)

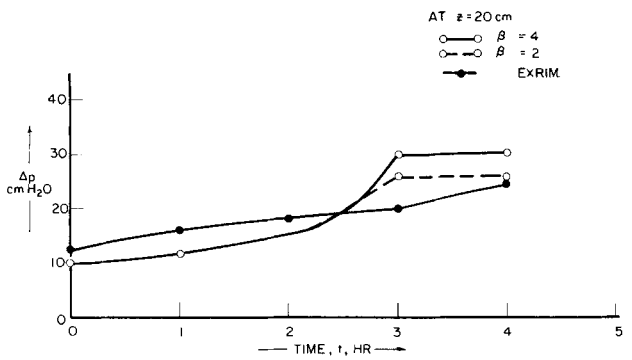

Fig. 6. Comparison of experimental and predicted values for pressure drop data (Ives, 1961).

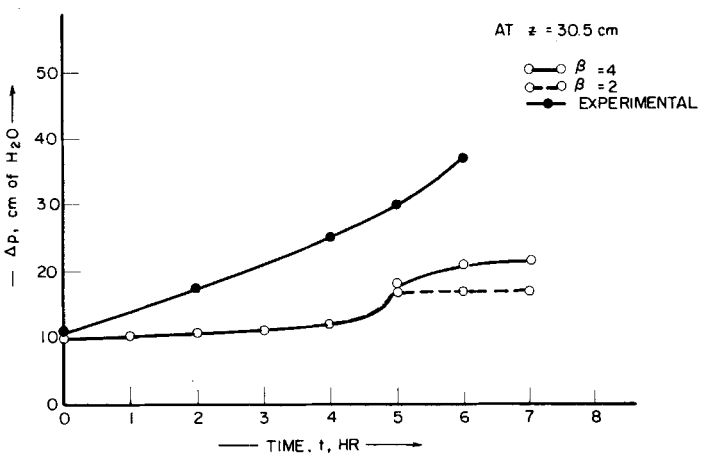

Fig. 8. Comparison of experimental and predicted values for pressure drop data (Deb, 1969).

The comparison with Deb's data is given in Figure 3 in the form of c vs. z at various times. Here the reversal of filtrate quality as observed in the experiment was confirmed in simulation. The increase in the value of β tends to reduce filtrate quality, although there is no definitive

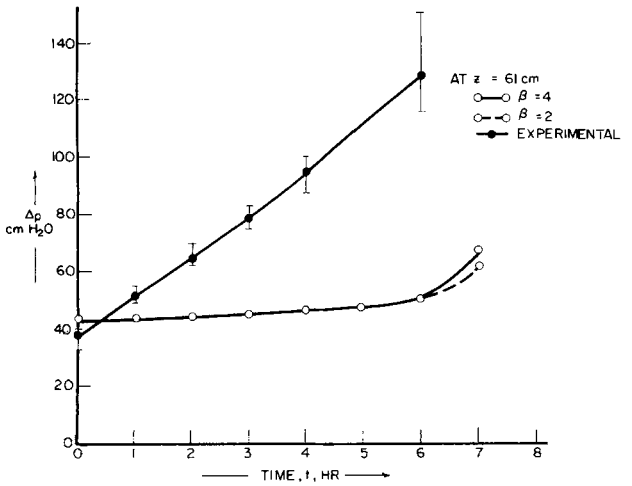

Fig. 9. Comparison of experimental and predicted values for pressure drop data (Rimer, 1968).

indication as to which assumed value results in better agreement. In the case of Camp's data, the prediction gives a sharper concentration profile than experiment (see Figure 5). However, it should be noted that Camp's experiment was performed using a graded filter bed, while the prediction was based on a uniform bed. This difference must account for at least part of the disagreement observed in the comparison.

The comparisons of the overall pressure drop are given in Figures 6, 7, 8, and 9. The comparison with Ive's results (Figure 6) showed that at the end of the run, the predicted value of Δp was found to be 30 ($\beta = 4$) or 26 ($\beta = 2$) as compared with the experimental value of 25 cm of water. This comparison, however, must be viewed as somewhat inconclusive, since the overall pressure drop is rather small. This is also true for Camp's data (Figure 7). The predicted pressure drop at the end of six hours of operation was found to be only slightly half of the experimental value in the case of Deb's data (Figure 8), but it is interesting to note that both the predicted curve of Δp vs. time and the experimental one turn out to consist of two parts, and the qualitative behavior of the second parts of the Δp vs. t curves are remarkably similar. The comparison with Rimer's data is given in Figure 9. However, had the transition of deposit morphology occurred at an earlier time (that is, smaller value of σ_{tran}), a much better agreement would result. In fact, the second part of the Δp (or ΔH) vs. time curve showed a great similarity to the experimental value. Even the experimental values exhibited a great deal of scatter in this case.

In general, the comparison indicates that simulation methods proposed in this work can be used to provide an order of magnitude estimate on a truly predictive basis. Furthermore, although the hypothesis used to formulate the method represents a highly simplified version of the actual phenomenon occurring in deep bed filtration, it is qualitatively consistent with experimental observation and takes into account the importance of the evolution of deposit morphology in the course of the filtration process. It is obvious that significant improvement of the present method can be made in several ways. A better specification of the values of σ_{tran} and β may be a possibility. Also, the evolution of deposit morphology may be taken to be more elaborate than the two-stage assumption made in this work, and a different and more accurate criterion could be established for the nonretentivity of filter bed. These improvements, however, cannot be made with further experiments performed under well-defined conditions. The importance of data gathered from a systematic program of critical experiments is self-evident.

ACKNOWLEDGMENT

This work was performed under Grant No. ENG 76-08755, National Science Foundation.

NOTATION

a = collector diameter in Happel's model, cm
a_p = particle radius, cm
A_s = group defined in Equation (38)
b = diameter of liquid shell, cm
c = concentration (v/v)
c_o = feed concentration (v/v)
d_c = constriction diameter, cm
d_g = grain diameter, cm
d_p = particle diameter, cm
g = gravitational acceleration
H = Hamaker constant ($\sim 1 \times 10^{-13}$ erg)
k = Boltzmann constant (1.38048×10^{-16} erg/°K)
l = length of the unit bed element, cm
L = length of the filter bed
N = number of constricted tubes per unit bed cross section, cm^{-2}
N_G = gravity group, defined in Equation (36)
N_{Lo} = London group, defined in Equation (34)
N_{Pe} = Peclet number, defined in Equation (37)
N_R = relative size group, defined in Equation (35)
p = defined in Equation (39)
P_{in} = pressure at bed inlet
p_{out} = pressure at bed outlet
S_{wi} = irreducible saturation
t = time, s
T = absolute temperature, °K
u = superficial velocity, cm/s
U = approach velocity, cm/s
V = interstitial velocity, cm/s
V_{cr} = critical interstitial velocity, cm/s
w = defined in Equation (40)
z = bed depth, cm

Greek Letters

α = parameter vector, see Equation (9)
β = parameter vector, see Equation (10)
β = correction factor the volume of deposited matter required to block one unit cell
Δp = pressure drop across a filter bed
ϵ = bed porosity
ϵ_d = deposit porosity
η = collection efficiency of the unit bed element
θ = corrected time, defined in Equation (4)
λ = filter coefficient
μ = viscosity of suspension
ρ = fluid density, g/cm^3
ρ_p = particle density, g/cm^3
σ = specific deposit, volume of deposited matter per unit bed volume
σ_{max} = maximum specific deposit
σ_{tran} = transition specific deposit
σ_{ult} = ultimate specific deposit corresponding to nonretaining stage

LITERATURE CITED

Camp, T. R., "Theory of Water Filtration," *Proc. ASCE, J. Sanitary Eng. Div.*, 90, No. SA4, 3 (1964).

Conley, W. R., and Kuo-ying Hsiung, "Design and Application of Multimedia Filters," *J. Am. Water Works Assoc.*, 61, 67 (1969).

Deb, A. K., "Theory of Sand Filtration," *Proc. ASCE, J. Sanitary Eng. Div.*, **95**, 399 (1969).
Herzig, J. P., D. M. Leclerc, and P. LeGoff, "Flow of Suspensions through Porous Media—Application to Deep Bed Filtration," *Ind. Eng. Chem.*, **62**, 8 (1970).
Hsiung, Kuo-ying, "Prediction of Performance of Granular Filters for Water Treatment," Ph.D. dissertation, Iowa State Univ., Ames (1967).
———, and J. L. Cleasby, "Prediction of Filter Performance," *Proc. ASCE, J. San. Eng. Div.*, **94**, No. SA4, 1043 (1968).
Huang, J. Y. C., and E. R. Bauman, "Least Cost Sand Filter for Iron Removal," *ibid.*, **97**, No. SA2, 171 (1971).
Hutchinson, H.P., and D. N. Sutherland, "An Open-Structure Open Solid," *Nature*, **206**, 1063 (1965).
Ives, K. J., "Rational Design of Filters," *Proc. Inst. Civil Engrs. (London)*, **16**, 189 (1960).
———, "Filtration Using Reduction Algae," *Proc. ASCE, J. Sanitary Eng. Div.*, **87**, No. SA3, 23 (1961).
———, "Simplified Rational Analysis of Filter Behavior," *Proc. Inst. Civil Engrs. (London)*, **25**, 345 (1963).
———, "Theory of Filtration," Special Lecture, No. 7 Int'l Water Supply Congress and Exhibition, Vienna (1969).
Maraudas, A., Ph.D. dissertation, London Univ., England (1961).
———, and P. Eisenklam, "Clarification of Suspensions: A Study of Particle Deposition in Granular Media. Part I—Some Observations on Particle Deposition," *Chem. Eng. Sci.*, **20**, 867 (1965).
———, "Part II—A Theory of Clarification," *ibid.*, 875 (1965).
Mohanka, S. S., "Theory of Multistage Filtration," *Proc. ASCE, J. Sanitary Eng. Div.*, **95**, SA6, 1079 (1969).
Payatakes, A. C., Chi Tien, and R. M. Turian, "A New Model for Granular Porous Media—Part I Model Formulation," *AIChE J.*, **19**, 58 (1973*a*).
———, "A New Model for Granular Porous Media—Part II Numerical Solution of Steady State Incompressible Newtonian Flow Through Periodically Constricted Tubes," *ibid.*, 67 (1973*b*).
Pendse, H., Chi Tien, and R. M. Turian, "Dispersion Measurement in Clogged Filter Beds—A Diagnostic Study on the Morphology of Particle Deposits," *AIChE J.*, **24**, 473 (1978).
Rajagopalan, R., and Chi Tien, "Trajectory Analysis of Deep Bed Filtration Using the Sphere-in-cell Porous Media Model," *AIChE J.*, **22**, 523 (1976).
———, "Single Collector Analysis of Collection Mechanisms in Water Filtration," *Can. J. Chem. Eng.*, **55**, 246 (1977).
Rimer, A. E., "Filtration Through a Trimedia Filter," *Proc. ASCE, J. Sanitary Eng. Div.*, **94**, SA No. 3, 521 (1968).
Spielman, L. A., and J. A. FitzPatrick, "Deposition of Non-Brownian Particles Under Colloidal Forces," *J. Colloid Interface Sci.*, **43**, 51 (1973).
Wnek, W. J., D. Gidaspow, and D. T. Wasan, "The Role of Colloidal Chemistry in Modelling Deep Bed Liquid Filtration," *Chem. Eng. Sci.*, **30**, 1035 (1975).
Yao, K.-M., M. T. Habibian, and C. R. O'Melia, "Water and Waste Water Filtration Concepts and Applications," *Environ. Sci. Technol.*, **5**, 1105 (1971).

Manuscript received February 20, 1978; revision received November 20, and accepted January 3, 1979.

A Gas Convection Model of Heat Transfer in Large Particle Fluidized Beds

A steady gas convection model of heat transfer to a horizontal cylinder immersed in a large particle gas fluidized bed has been developed. The model is based upon the hypothesis that the large particles will be isothermal and includes the effect of radiation as well as interstitial turbulence.

Results of calculations based on the model, for a two-dimensional bubbling bed, indicate that a single bubble, having a diameter equal to the cylinder diameter, has a relatively small influence on the total heat transfer.

RONALD L. ADAMS
and
JAMES R. WELTY
Department of Mechanical Engineering
Oregon State University
Corvallis, Oregon 97331

SCOPE

Fluidized bed combustion is currently being studied intensively since beds containing limestone or dolomite will adsorb sulfur dioxide, thereby providing a way to burn high sulfur coals to generate power while maintaining air quality standards. The atmospheric pressure fluid bed combustor is expected to operate at a temperature of about 1 100°K and contain particles with mean diameters as large as 6 mm. Current heat exchanger designs are based on horizontal tube arrangements, so heat transfer to horizontal cylinders either singly or in banks immersed in a large particle bed is of interest.

Heat transfer to surfaces immersed in a large particle fluidized bed such as the atmospheric combustor is expected to occur principally by gas convection. Accordingly, a gas convection heat transfer model has been developed considering the flow within interstitial voids adjacent to the surface as well as within bubbles contacting the surface. Radiation heat transfer from the hot particles, important at combustion temperatures, is also included, and the effect of interstitial turbulence is incorporated in the convection model. Most previous models of fluid bed heat transfer were developed for beds containing small particles in which unsteady conduction is the dominant mode of heat transfer and are considered inadequate for the analysis of heat transfer to a horizontal cylinder immersed in a large particle bed in which gas convection is the dominant mode of heat transfer.

Ronald L. Adams is with Massachusetts Institute of Technology Lincoln Laboratory, P.O. Box 73, Lexington, Mass. 02173.